The Meteoritical Society

Meteoritics & Planetary Science 44, Nr 1, 3–14 (2009)
Abstract available online at http://meteoritics.org

K-Ar dating of rocks on Mars: Requirements from Martian meteorite analyses and isochron modeling

Donald D. BOGARD

ARES, Code KR, NASA Johnson Space Center, Houston, Texas 77058, USA
*Corresponding author. E-mail: donald.d.bogard@nasa.gov

(Received 29 April 2008; revision accepted 17 July 2008)

Abstract–Radiometric age dating of Martian rocks and surfaces at known locations for which crater densities can be determined is highly desirable in order to fully understand Martian history. Performing K-Ar age dating of igneous rocks on Mars by robots, however, presents technical challenges. Some of these challenges can be defined by examining Ar-Ar data acquired on Martian meteorites, and others can be evaluated through numerical modeling of simulated K-Ar isochrons like those that would be acquired robotically on Martian rocks. Excess ^{40}Ar is present in all shergottites. Thus for Martian rocks, the slopes of K-Ar isochrons must be determined to reasonable precision in order to calculate reliable ages. Model simulations of possible isochrons give an indication of some requirements in order to define a precise rock age: Issues addressed here are: how many K-Ar analyses should be made of rocks thought to have the same age; what range of K concentrations should these analyzed samples have; and what analytical uncertainty in K-Ar measurements is desirable. Meteorite data also are used to determine the D/a^2 diffusion parameters for Ar in plagioclase and pyroxene separates of several shergottites and nakhlites. These data indicate the required temperatures and times for heating similar Martian rocks in order to extract Ar. Quantitatively extracting radiogenic ^{40}Ar could be difficult, and degassing cosmogenic Ar from mafic phases even more so. Considering all these factors, robotic K-Ar dating of Martian rocks may be achievable, but will be challenging.

INTRODUCTION

Processes and geological features on the Martian surface have associated ages which define Martian history. In general, the times of these processes and features are poorly known, and we would like to determine them more accurately. Relative Martian surface ages are estimated by measuring crater densities. But, lacking a single directly dated Martian surface, these ages must be extrapolated from the lunar crater data, and they also contain uncertainties associated with primary versus secondary craters and erosion of and deposition on Martian surfaces (Hartmann and Neukum 2001). Martian meteorites generally have precisely determined radiometric ages (e.g., Nyquist et al. 2001), but their original locations on Mars are unknown, and therefore they cannot calibrate crater densities. An apparent conflict between Martian crater densities, which indicate most Martian surfaces are old, and Martian meteorite ages, which are mostly young, was pointed out by Nyquist et al. (1998). Return of Martian rocks to Earth for radiometric dating could furnish a calibration point for relative surface ages. But, sample return is likely to be a complex and expensive mission and will not occur for many years. For some time, many individuals have considered the possibilities of age dating Martian surface rocks by robotic spacecraft. Martian missions currently being considered or constructed (e.g., the Mars Science Lander) have the capability, in principle, to measure concentrations of K and Ar in surface samples and may be able to determine rock ages.

The K-^{40}Ar dating technique is thought by many to be the simplest to implement by robots. Determination of K concentrations in rocks may be straightforward for robotic missions. However, studies of Martian shergottites have shown that it is often difficult to resolve ^{40}Ar produced by in situ ^{40}K decay from other ^{40}Ar components present. Almost all ^{39}Ar-^{40}Ar age analyses of Martian shergottites give "ages" that are older, some much older, than the Sm-Nd formation ages. For example, the apparent K-Ar ages, based on total K and ^{40}Ar measured in Ar-Ar dating at JSC (Johnson Space Center) of many Martian meteorites, ranges from 250 Myr for a plagioclase separate of the Zagami shergottite to 6,000 Myr for an impact glass inclusion from the Elephant Moraine

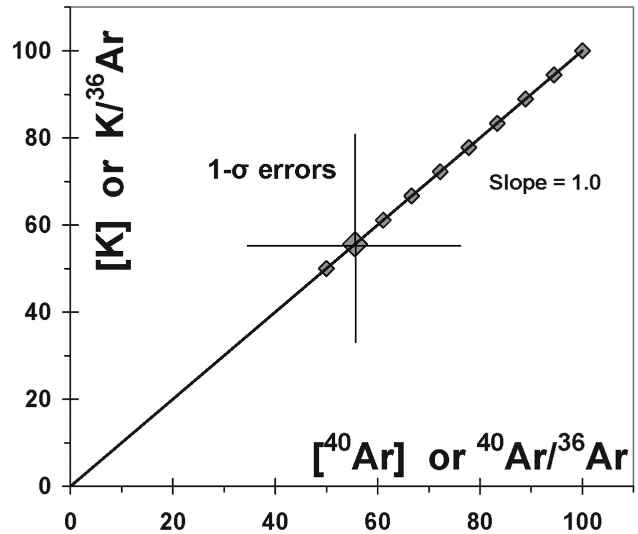

Fig. 1. Schematic of assumed isochron of slope one used to simulate K-Ar isochrons for Martian rocks. This example assumes 10 rock analyses with K concentrations spread evenly over a factor of two. Each K and Ar is assumed to have a one-sigma uncertainty proportional to the K and Ar contents, as indicated for one point.

(EET) A79001 shergottite. Yet, the Sm-Nd formation age of both these meteorites is ~170 Myr (Nyquist et al. 2001). Excess ^{40}Ar components in shergottites can be shock-implanted from the Martian atmosphere (Bogard and Johnson 1983; Marti et al. 1995; Bogard and Garrison 1998a; Walton et al. 2007) or acquired from the parent magma (Bogard and Park 2008a, 2008b). In addition, Martian surface rocks, like Martian meteorites, can contain multiple ^{36}Ar components, including cosmogenic Ar, Martian atmospheric Ar, and Martian interior Ar. These various ^{36}Ar components often are not correlated within the sample, and their presence will cause an isochron plot of ^{40}Ar/^{36}Ar versus K/^{36}Ar to scatter,. The absence of reactor-produced Ar isotopes (^{39}Ar and ^{37}Ar), available in the ^{39}Ar-^{40}Ar technique, means there may be no easy method of resolving these ^{36}Ar components in robotic dating (Bogard and Park 2008a).

Bogard and Park (2008a, 2008b) show that excess ^{40}Ar varies by a relatively small amount among mineral separates from many shergottites of various types and showing different formation ages and shock levels. This excess ^{40}Ar is not Martian atmosphere. When the K concentrations obtained in these analyses, which vary by two orders of magnitude, are plotted against the total ^{40}Ar concentrations obtained in the same analyses, shergottites having the same Sm-Nd age define a narrow isochron band, which is consistent with the Sm-Nd age and the presence of ~1–2 × 10^{-6} cm^3/g excess ^{40}Ar in each sample. One cannot presume that rocks robotically dated on Mars will not contain excess ^{40}Ar, either from the interior or atmosphere, which would cause the apparent age to be too old. The presence of excess ^{40}Ar would mean that isochron plots of

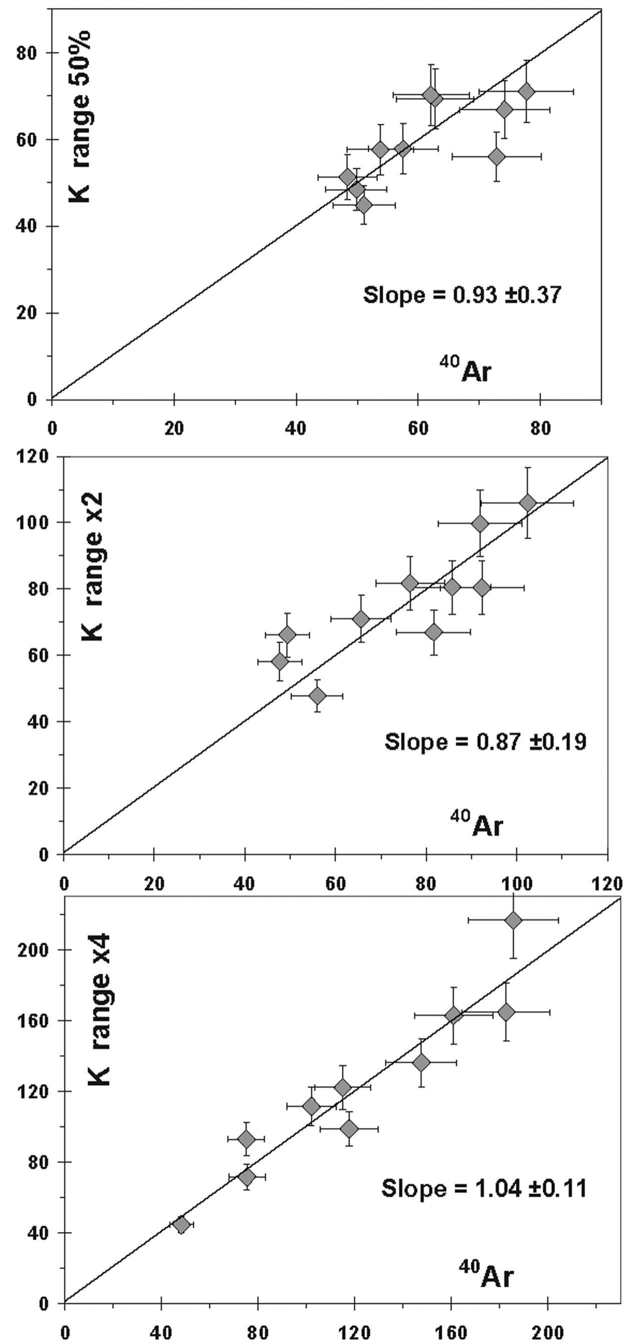

Fig. 2. Examples of possible K-Ar isochrons that could be observed for Martian rocks, assuming starting conditions shown in Fig. 1. These three isochrons all assume 10 K-Ar analyses evenly spread over a range in K of 50%, a factor of 2, and a factor of 4 (top to bottom) and analytical measurement uncertainties of ±10%, proportional to K and Ar concentration. Data for each isochron were obtained by a random number generator that gave a Gaussian distribution of individual points, given the K concentration and uncertainty as input parameters for each starting point. The slope for each isochron is indicated and was obtained using the Williamson (1968) data fit, which weighs each point by its individual uncertainties.

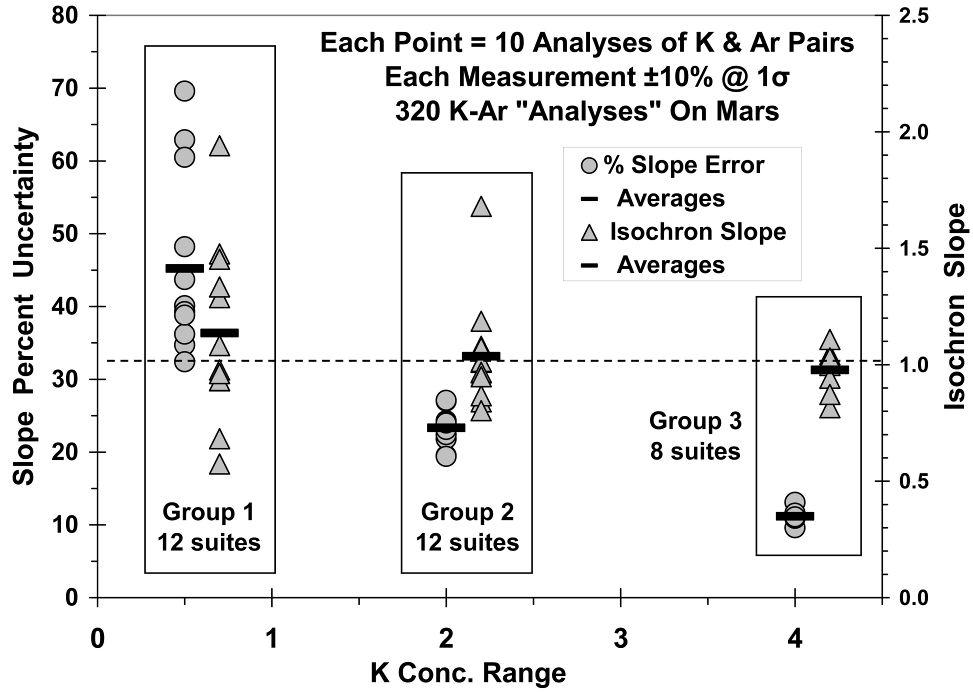

Fig. 3. Results of Gaussian analyses of 32 sample suites, simulating 320 measurements of K-Ar pairs on Martian rocks, plotted against the range in K concentrations assumed (50%, ×2, and ×4). Each symbol represents a single Gaussian result, like the examples in Fig. 2. The resulting slopes and the percent 1σ uncertainties in those slopes, obtained by Williamson (1968) data fits, are indicated separately for each group of Gaussian analyses. The horizontal bars indicate averages.

the data would not pass through the origin. Thus, data produced by robotic K-Ar dating of Martian rocks should be examined in two types of isochron plots, $^{40}Ar/^{36}Ar$ versus K/^{36}Ar and K versus total ^{40}Ar. An isochron normalized to ^{36}Ar works best when the trapped $^{40}Ar/^{36}Ar$ ratio is constant, as in many terrestrial samples, and an isochron not normalized appears to work best for shergottites, where the trapped ^{40}Ar concentration is nearly constant and the trapped ^{36}Ar is poorly defined. The situation may also exist for some Martian rocks that neither of these conditions are met and an isochron cannot be defined.

Many experiments of Ar-Ar dating of Martian meteorites have been reported in the literature (Some examples of more recent reports are Turner et al. 1997; Bogard and Garrison 1999; Swindle and Olson 2004; Walton et al. 2007; Bogard and Park 2008a). Other reports have addressed the $^{40}Ar/^{36}Ar$ ratio in trapped Martian interior argon (e.g., Terribilini et al. 1998; Mathew and Marti 2001; Schwenzer et al. 2007). Some of the issues involved in making K-Ar age determinations on Mars were discussed by Swindle (2001). Some requirements for successfully dating rocks on Mars robotically can be quantified, using both the extensive argon diffusion data obtained by the JSC lab on Martian meteorites, and by analyses of numerically simulated isochron plots. That is the purpose of this paper, which uses Ar diffusion data from Martian meteorites to examine heating requirements to quantitatively degas Ar from samples, and which examines the required variation in K concentrations among rocks of the same age and required precision of K and ^{40}Ar analyses needed to yield precise isochron ages. Rocks similar to Martian meteorites may be common on Mars (McSween 1994, 2002). Thus, these evaluations should be of value to future mission activities that attempt K-Ar dating on Mars. If such robotic dating efforts prove unsuccessful, the incentive for sample return and radiometric dating of Martian rocks in terrestrial labs increases.

SIMULATED K-Ar ISOCHRONS

I have numerically simulated isochrons that could be obtained from a series of robotic K and Ar analyses of Martian rocks that may possess the same formation age. To achieve a desirable precision in a K-Ar isochron age, this modeling addresses the following questions. What range of K concentrations among samples is needed; how many sample analyses should be made; and what is the effect on the isochron of analytical precision in those analyses? This modeling examines only random errors that are produced in measuring K and Ar concentrations, and does not consider any systematic errors that may be present.

Figure 1 is an idealized K-Ar isochron, either normalized to ^{36}Ar or not, which presumes 10 analyses of K-Ar pairs for one or more Martian rocks believed to possess a common age. Ten K-Ar analyses would seem to be an achievable number, but both 5 and 20 data pairs also will be

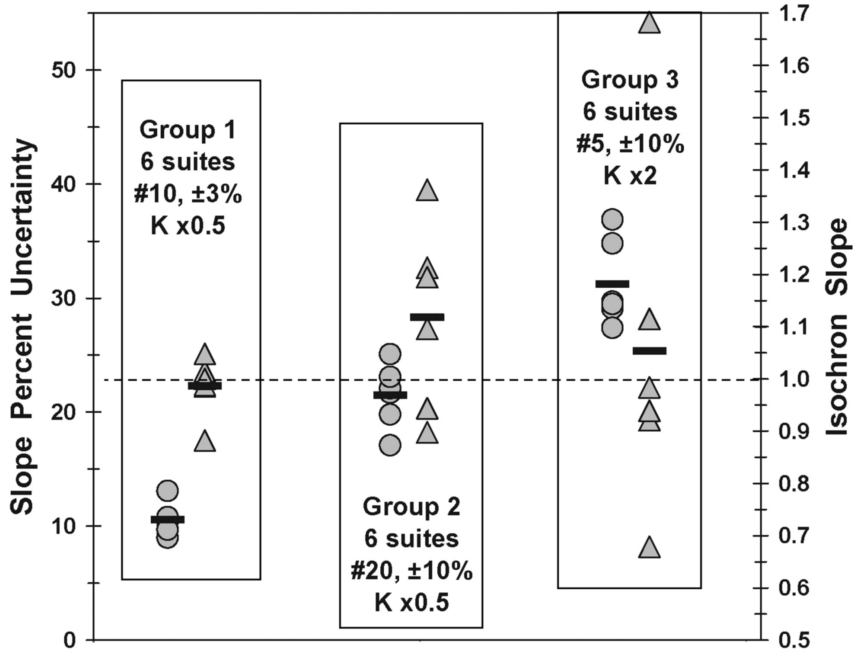

Fig. 4. Results of Gaussian analyses with three different starting assumptions. Group 1 represents 6 suites of 10 samples each, a K range of 50%, and individual uncertainties of ±3%. Group 2 represents 6 suites, a K range of 50%, individual uncertainties of ±10%, and with 20 K-Ar analyses per suite, rather than 10. Group 3 represents 6 suites of 10 samples each, a K range of ×2, ±10% individual uncertainties, but with only 5 K-Ar analyses per suite. Mean values are indicated by horizontal bars. Symbols as in Fig. 3.

examined. Figure 1 further assumes that K in these 10 samples varies uniformly by a factor of two and that the true isochron slope has a value of one. The same one-sigma measurement error is assigned to each K and Ar analysis, where the error is proportional to the concentration. Different ranges of K and measurement uncertainties of ±10% and ±3% will be considered. For each K-Ar pair in these 10 analyses, I used a random number generator and a mathematical Gaussian extraction (Anonymous 2008; Carter 2008) to produce ten K-Ar data pairs, one for each starting K-Ar pair shown in Fig. 1. This math routine produces a distribution of K and Ar values that is a sub-set of a Gaussian distribution about the isochron of slope one. A Gaussian distribution is the likely form of K and Ar data one would see from random errors in analytical measurements. Both the mean and the standard error of the Gaussian distribution of each data pair is entered as a variable into the math routine. The validity of this math routine was checked by having it generate a large number of data, whose distribution showed the expected mean value and standard deviation entered into the Gaussian routine.

Figure 2 shows the K-Ar data pairs and their distribution about the original isochron resulting from three different Gaussian numerical simulations, one each for the case that K varies by 50%, a factor of 2, or a factor of 4. Each time the Gaussian routine is run, a different distribution of 10 K-Ar pairs is produced about the original isochron of slope one, and Fig. 2 represents but three examples. Each of these simulated analyses would represent a suite of possible K-Ar analyses on the Martian surface of 10 samples having the same age. For each simulated analysis, I calculated the slope of the resulting isochron (Fig. 2) using the Williamson (1968) data fit, which weighs each K-Ar pair by their assigned uncertainties (±10% in Fig. 2). The isochron age would be directly proportional to the isochron slope. As shown below, the magnitude by which these slopes deviate from the starting isochron slope of one depends on the range of K concentrations and the assumed measurement uncertainties in K-Ar pairs. Obviously, if 10 such samples all possessed the same K, an isochron cannot be defined.

The numerically generated Gaussian analyses shown in Fig. 2 represent but some examples among many possibilities as to the distribution of measured K-Ar data pairs and the isochron slope they define. Thus, for each set of starting assumptions, multiple sets of isochrons were generated using the Gaussian routine. Figure 3 plots the isochron slope and the uncertainty in that slope for multiple Gaussian suites of 10 samples, where each K and Ar datum has an analytical uncertainty of ±10%. I generated 12 suites for a K variation of 50%, 12 suites for a K variation of ×2, and 8 suites for a K variation of ×4. The 32 symbols plotted in Fig. 3 simulate 320 analyses of K-Ar pairs on Mars. Note that the results obtained do not depend on the magnitude of the K concentration, but only on the range in K concentrations across a sample suite.

The precision of the isochron slope and age dramatically increases as the range in K content increases (Fig. 3). For a

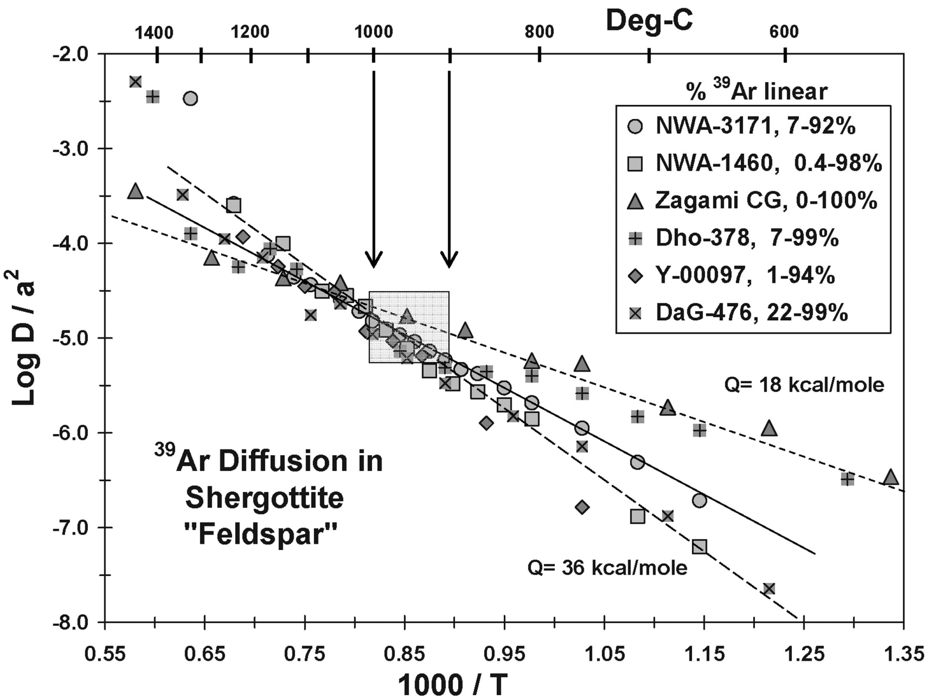

Fig. 5. Arrhenius plot of D/a^2 versus reciprocal temperature in degrees Kelvin, times 1000 (bottom scale) and °C (top scale), as calculated from stepwise temperature degassing of ^{39}Ar from plagioclase separates of six shergottites. The fractions of total ^{39}Ar release that define linear trends are indicated in the legend. Activation energies for trends with the least slope (Zagami) and largest slope (Northwest Africa [NWA] 1460) are given. The Ar diffusion distance, a, is probably similar to the grain size for these separates of 74–149 microns. The two vertical arrows define the log D/a^2 values for heating temperatures of 900–1000 °C as −5.2 to −4.5.

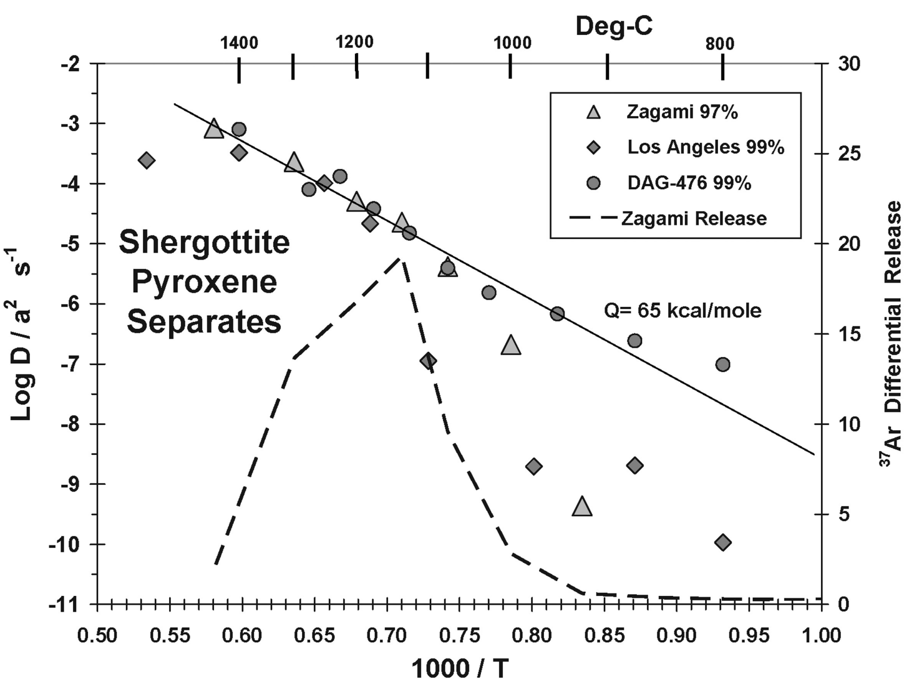

Fig. 6. Arrhenius plot of D/a^2 versus reciprocal temperature in degrees Kelvin, times 1000 (bottom scale) and °° (top scale), as calculated from stepwise temperature degassing of ^{37}Ar from pyroxene separates of three shergottites. The fractions of total ^{39}Ar release plotted are 97–99%. The dashed line shows the differential release rate of ^{37}Ar from Zagami pyroxene in arbitrary units (right Y-axis).

total K variation of 50% across 10 samples in a suite, 12 suites of samples in Group 1 give slopes that vary from 0.5 to 2.0, compared to the original slope of 1.0. The average of these 12 slopes is 1.136, which demonstrates that an analysis of 120 samples gives better accuracy than analysis of only 10 (one suite). The 1σ uncertainties in these slopes also show a wide range of ~32–70%. In general, the uncertainty in an individual slope increases as the slope increasingly deviates from the starting slope of one. If these modeled data suites represented analyses of actual Martian rocks, the random uncertainty in derived isochron ages for a suite of 10 samples would be about a factor of two. For a range in K concentrations less than 50%, one could expect a greater age uncertainty than for a K variation of 50%.

For Gaussian data sets with a total variation in K concentrations of ×2, 12 suites of samples in Group 2, with one exception, give slopes of 0.80–1.19, compared to the starting slope of 1. One sigma uncertainties in these slopes vary by 19–27%. Increasing the range of K concentrations of analyzed samples by a factor of two significantly increased the accuracy and precision of the derived isochron slope. However, there still exists the low possibility that a significantly deviant isochron slope might be obtained (e.g., Group #2). The mean slope of these 12 suites is 1.036. It is interesting to note that among Group 2, the analysis that gives a slope of 1.6 only gives a 1σ uncertainty of ±24%. This demonstrates that for an occasional sample suite, the slope uncertainty may not be an adequate measure of the deviation of the data from the true slope, just as in any Gaussian distribution of data, one expects ~5% of the values to fall outside the 2σ error.

For a total K variation of ×4 for 10 samples in a suite, 8 suites of samples in Group 3 gave slopes of 0.815 to 1.108, with a mean slope of 0.978. Individual uncertainties in these slopes vary by ~10–13%, which is similar to the assumed ±10% uncertainties in K-Ar analysis pairs. With 10% analytical measurement uncertainties, increasing the total range in K concentrations from ×2 to ×4 is not likely to significantly increase the precision by which isochron slopes are defined. From these simulated analyses, we conclude that to achieve K-Ar isochron ages on Mars to a reliability of a few tens of percent, a suite of approximately 10 samples must vary in total K concentration by a factor of two or greater, if analytical measurement precision of K and Ar are ±10%.

Figure 4 plots three additional groups of Gaussian analyses of sample suites. Group 1 shows six sample suites, each with 10 samples and having a total range in K of 50%, but with assumed analytical precision in the K and Ar measurements of ±3%. The slopes of these suites are 0.88–1.05, with an average of 0.986, and uncertainties in the slope vary 9–13%. Decreasing the analytical uncertainties in measuring K and Ar concentrations, while other parameters remained the same, increased the precision and reliability of the derived isochron slopes by at least a factor of three. Thus, one way to compensate for a relatively small range of total K among Martian rocks being dated is to increase analytical measurement precision.

Group 2 of Gaussian suites in Fig. 4 utilized 20 analyses of K-Ar pairs per suite, possessing analytical uncertainties of ±10% and a total K variation of 50%. Six such Gaussian analyses gave slopes of 0.89–1.36 (average 1.12) and 1σ slope uncertainties of 17–25%. Doubling the number of analyses in a sample suite significantly increases the accuracy of the slope and its precision, although by a smaller factor than decreasing the individual analytical precision. Group 3 plotted in Fig. 4 shows six sample suites, each with only 5 samples and possessing a total range in K of a factor of two and analytical precision in the K and Ar measurements of ±10%. Comparing Groups 2 and 3, we note that decreasing the number of samples analyzed in a suite from 10 to 5 did decrease the accuracy and precision of the isochron slope, as would be expected. Again, one suite in Group 3 gives a slope whose deviation from the starting slope of one lies well outside the slope error.

All of these simulated isochrons assume that all samples in a suite of Martian samples possess the same age and similar concentrations of excess, trapped ^{40}Ar, as apparently is the case for many shergottites (Bogard and Park 2008b). Alternatively, the amount of trapped ^{40}Ar could be very low and the isochron could pass near the origin. If one or more samples in a suite of samples contained significant concentrations of Martian atmospheric ^{40}Ar, as is observed in impact glass in some shergottites, then that sample could be expected to deviate significantly from the isochron slope defined by the other samples and it could be discarded from the isochron fit.

ARGON DIFFUSION IN MARTIAN METEORITES

Robotic spacecraft have limited power output, whereas degassing Ar from Martian rocks will require a significant amount of heat. For the JSC laboratory, we typically heat samples for times of 20 min at each of many temperature steps in a deep-well furnace equipped with a thermocouple for precise temperature measurement. These conditions are ideal for determining Ar diffusion characteristics from the data acquired in Ar-Ar dating. For plagioclase samples, the Ar diffusion rate is determined from ^{39}Ar, which is produced in the reactor in the same lattice sites that contain ^{40}Ar from radiogenic ^{40}K decay, and thus the two isotopes should possess the same diffusion characteristics. For pyroxene, I use ^{37}Ar, which is produced in the reactor from Ca and resides in both pyroxene and plagioclase, as does cosmogenic Ar. The rate at which Ar is lost from silicate material depends on the Ar diffusivity, D, in that material, the diffusion distance, a, and the temperature and time of sample heating. Calculation of the diffusion parameter, D/a^2, requires only the relative concentrations of ^{39}Ar and ^{37}Ar released for each temperature step, and the heating time for each step (Lagerwall and Zimen

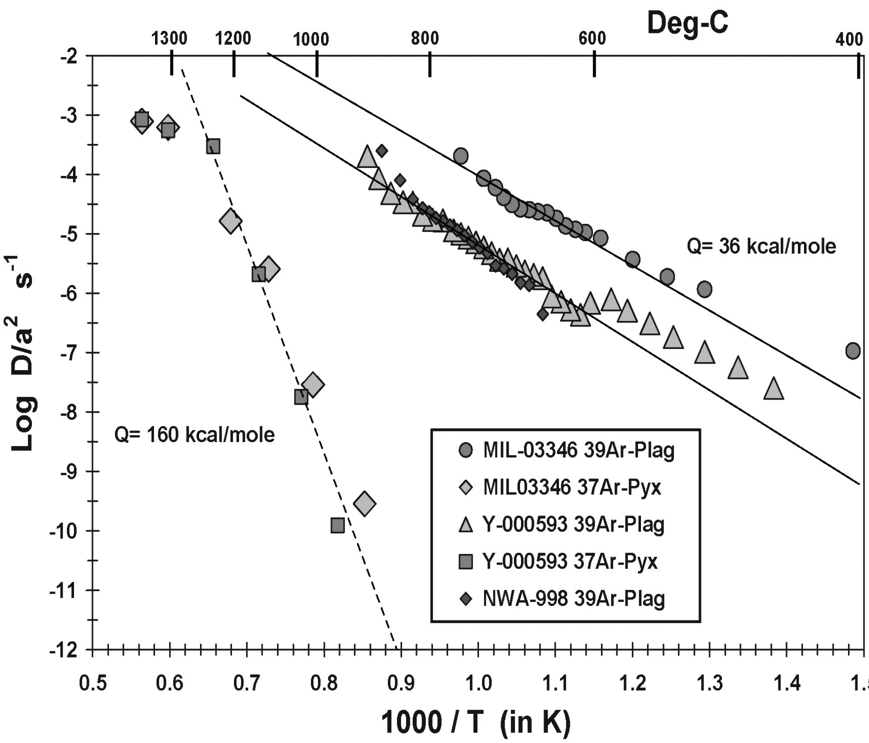

Fig. 7. Arrhenius plot of D/a² versus reciprocal temperature in degrees Kelvin, times 1000 (bottom scale) and C° (top scale), as calculated from stepwise temperature degassing of ^{39}Ar from plagioclase separates of nakhlites Miller Range (MIL) 03346, Yamato-000593, and NWA 998, and ^{37}Ar from pyroxene separates of MIL 03346 and Yamato-000593.

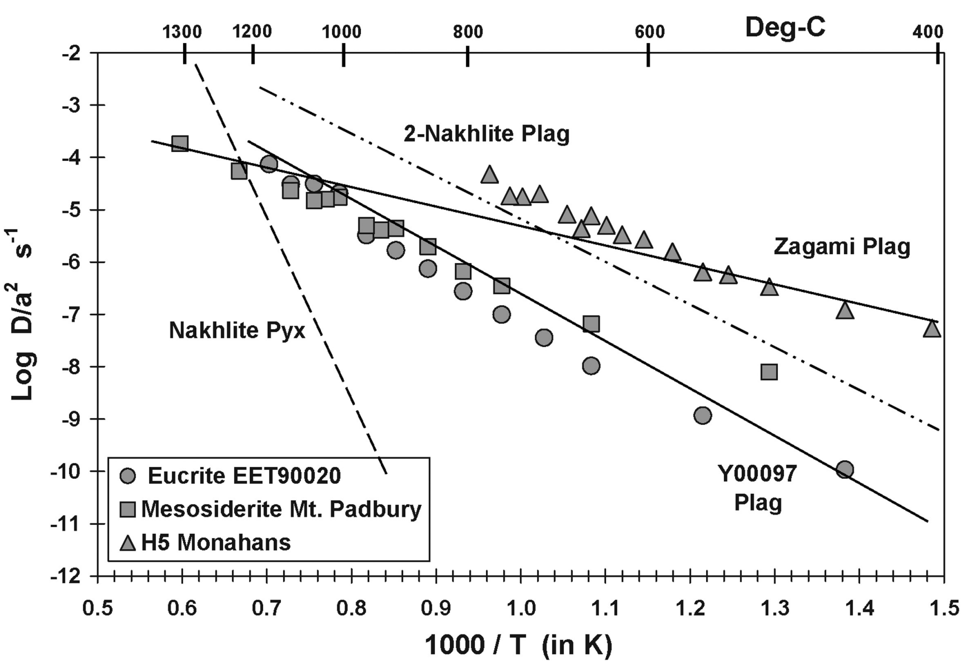

Fig. 8. Comparison of Ar diffusion data presented here for shergottites and nakhlites with ^{39}Ar diffusion data calculated from Ar-Ar analyses of a eucrite, a mesosiderite, and a H-5 chondrite. Lines are labeled according to sample and represent data trends from Figs. 5–7. Symbols represent non-Martian meteorites shown in the legend.

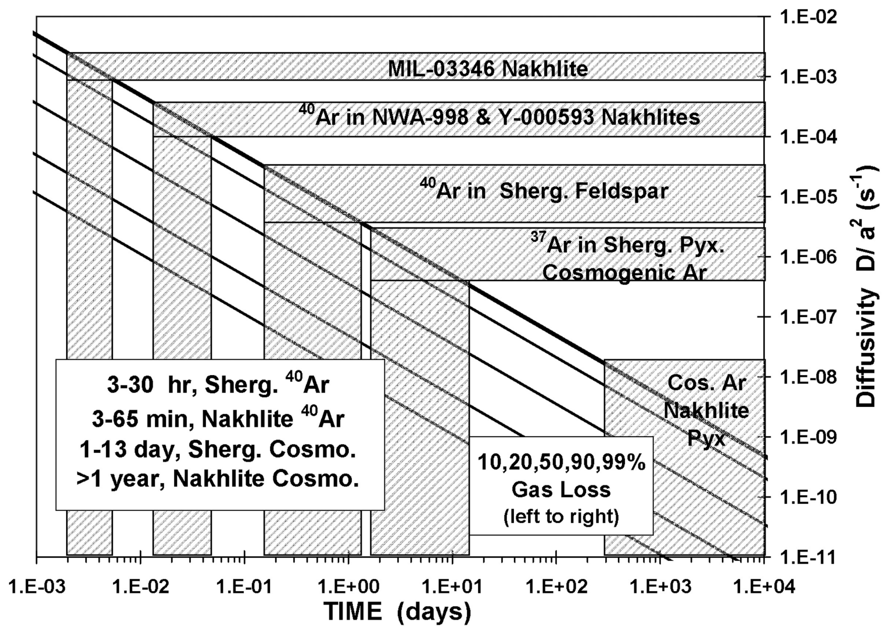

Fig. 9. Values of D/a^2 plotted against heating time (days) required to achieve various percentages of gas loss by diffusion, as indicated by the diagonal lines. The horizontal bands are defined by the D/a^2 values of ^{39}Ar diffusion in plagioclase separates of five shergottites (one middle band), ^{39}Ar diffusion in plagioclase separates of three nakhlites (upper two band bands), ^{37}Ar diffusion in pyroxene separates of three shergottites, and ^{37}Ar diffusion in two nakhlite pyroxenes (lowest band), for heating temperatures between 900 °C and 1000 °C. To achieve 99% degassing of Ar in this temperature range, each of these sample types would have to be heated for times of ~3–30 h (shergottite plagioclase), ~3–65 min (nakhlite plagioclase), 1–13 days (shergottite pyroxene,) and ≥1 yr (nakhlite pyroxene).

1964; Fechtig and Kalbitzer 1966; Bogard and Park 2008a). Thus, these diffusion data can be used to address the question of how much heating of Martian rocks would be required to quantitatively degas their Ar. We have determined Ar diffusion characteristics on several Martian meteorites, both whole rock and mineral separates. Some of the Ar isotopic data from which these diffusion data are obtained have been published (Park et al. 2007; Bogard and Park 2008a, 2008b; Misawa et al. 2008), but most have not. In this section, I first present Ar diffusion data acquired on plagioclase and pyroxene separates of several Martian meteorites. In the following section, I then use this diffusion data to infer single-step, heating temperatures and times for quantitative extraction of both radiogenic and cosmogenic Ar from rocks resembling Martian shergottites and nakhlites.

Figure 5 presents an Arrhenius diagram of the D/a^2 diffusion parameter for ^{39}Ar plotted against reciprocal temperature in Kelvin, multiplied by 1000 for ease in plotting. The data shown were acquired on plagioclase separates of six Martian shergottites, four classed as basaltic, one as lherzolitic (Yamato [Y-] 000097), and one as olivine phyric Dar al Gani (DaG) 476). Their Sm-Nd ages range over ~160–470 Myr. Their shock levels, where known, range from ~29 GPa for Zagami and DaG 476 (Fritz et al. 2005) to >55 GPa for Dhofar 378 (Ikeda et al. 2006). These mineral separates were prepared by C-Y Shih at JSC for radiometric dating and have a grain size range of 74–149 microns (100–200 mesh). Each of these six samples defines a strongly linear trend across a large majority of its ^{39}Ar release, indicating relatively simple Ar diffusion characteristics from a single phase. For a few meteorites (Zagami, NWA 1460, and Y-00097) the linear diffusion trend includes the earliest release of ^{39}Ar from grain surfaces. For three other hot desert meteorites, however, early release of ^{39}Ar probably derived from strongly weathered grain surfaces, and we have not included these data in the diffusion calculations. The percentages of total ^{39}Ar release that define the linear portion of the Arrhenius plots for these samples range over 77–100% and are indicated in the Fig. 5 legend.

All six Arrhenius plots in Fig. 5 intersect at a temperature of ~1050 °C and narrowly define a value for D/a^2 at that temperature. Because plagioclase having Ab/An ratios typical of shergottites melts at temperatures above 1200 °C, deviation of three points from the Arrhenius trends at highest temperatures is attributed to Ar diffusion out of melted feldspar, where diffusion distances become greater. The activation energies calculated from the slopes of these data trends range from 18 kcal/mole for Zagami to ~40 kcal/mole for Y-00097. Activation energies are a measure of the resistance of the mineral lattice to gas diffusion as a function of temperature. Even larger variations in activation energies than reported here have been reported for meteorite groups of similar type (e.g., ordinary chondrites, Turner et al. 1978; mesosiderites, Bogard and Garrison 1998b). Presumably for all such samples, plagioclase is the major K-bearing mineral. The specific reasons for such variations have not been evaluated in detail.

Figure 6 gives Arrhenius plots for diffusion of ^{37}Ar in pyroxene separates of three shergottites. Again, these mineral separates were prepared by C.-Y. Shih at JSC for radiometric dating and have a grain size range of 74–149 microns. Whereas radiogenic ^{40}Ar from the decay of ^{40}K resides mainly in feldspar, cosmogenic ^{36}Ar and ^{38}Ar are produced from Ca and Fe in both mafic and feldspathic phases during GCR irradiation. Thus, Fig. 6 gives typical diffusion characteristics of cosmogenic Ar in shergottite pyroxene. These Arrhenius plots are not as well defined as those for feldspar (Fig. 5). Nevertheless, ^{37}Ar diffusion in pyroxene suggests a higher activation energy of ~65 kcal/mole. The majority of ^{37}Ar in all three samples released at temperatures above 1000 °C, as demonstrated by the ^{37}Ar differential release curve for Zagami pyroxene (Fig. 6). The figure legend indicates for each sample the percentage of total ^{37}Ar release that is plotted in Fig. 6. For those extractions releasing most of the ^{37}Ar, all three shergottites give very similar, linear diffusion trends. The reason for deviation of ^{37}Ar from these diffusion trends for intermediate temperature extractions of Zagami and Los Angeles is not clear, but these extractions represent a minor part of the total ^{37}Ar released. For Los Angeles Pyx, 85% of the total ^{37}Ar released at temperatures above 1150 °C. In contrast, the Arrhenius plot for DaG 476, classed as an olivine phyric, shows linearity to considerably lower temperatures and is defined by 99% of the total ^{37}Ar. Note that the D/a^2 value for ^{37}Ar diffusion in pyroxene at 1000 °C, ~10^{-6} per second, is more than an order of magnitude slower than diffusion of ^{39}Ar from plagioclase at the same temperature (Fig. 5). Thus, it requires more heating to quantitatively release cosmogenic Ar from shergottites, as compared to ^{40}Ar.

Figure 7 gives Arrhenius plots for diffusion of ^{39}Ar in plagioclase separates for the three nakhlites MIL 03346, Y-000593, and NWA 998, and of ^{37}Ar in pyroxene separates for MIL 03346 and Y-000593. The grain size range of these separates was 74–149 microns. The data shown for ^{37}Ar in pyroxene comprise 99% of the total ^{37}Ar released, give surprisingly high activation energies of ~160 kcal/mole, and show log D/a^2 values at 1000 °C of −8, which is considerably lower than D/a^2 for ^{37}Ar diffusion in shergottite pyroxene (Fig. 6). The plotted D/a^2 values for temperatures ≥1300 °C represent a minor amount of the total ^{37}Ar and may represent Ar degassing after melting begins. Diffusion plots of ^{39}Ar in the Y-000593 and NWA 998 plagioclases largely overlap, but D/a^2 values of MIL 03346 plagioclase are about a factor of 10 higher at a given temperature. Most D/a^2 data for all three nakhlite plagioclases give similar activation energies of ~36 kcal/mole, which is also similar to activation energies of some shergottites (Fig. 5). Release of ^{39}Ar in these three nakhlites is more complex than that of the shergottites shown

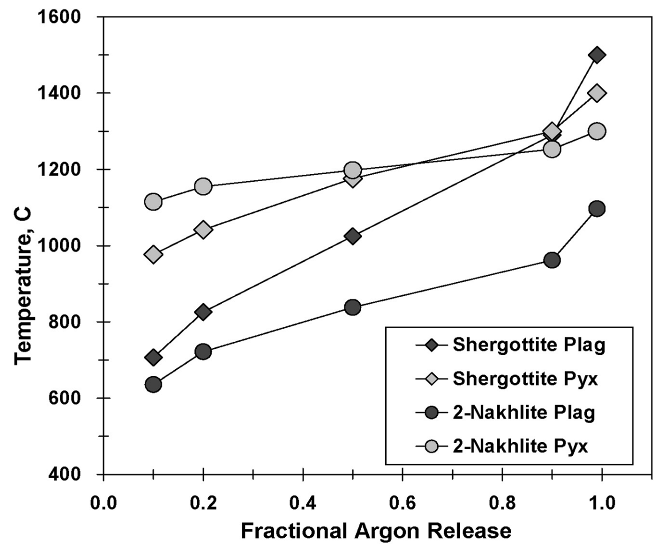

Fig. 10. Model-predicted fractional Ar release plotted against heating temperature for an arbitrary heating time of 15 min.

in Fig. 5. The nakhlite Ar release pattern suggests a second, minor K-bearing phase releasing at higher temperatures, which may be plagioclase encapsulated by pyroxene. The data shown for plagioclase in Fig. 7 do not consider these higher temperature data, but they still represent 80%, 90%, and 70% of the total ^{39}Ar released from MIL 03346, Y-000593, and NWA 998, respectively. In addition, argon isotopes released in the first few extractions of NWA 998 (6% of the ^{39}Ar) show effects of terrestrial weathering, and these data were not included in calculating D/a^2 values. Further, the first ~9% of the ^{39}Ar released from Y-000593 plot slightly above, but parallel to the trend defined by the rest of the data, and may represent a grain surface effect. Nevertheless, the D/a^2 values for the majority of the ^{39}Ar released from the three plagioclases across a wide temperature range appear to be well defined.

The D/a^2 data for nakhlite plagioclase extrapolated to 1000 °C indicate that ^{39}Ar diffusion from nakhlite plagioclase is faster compared to shergottite plagioclase by factors of ~10 for Y-000593 and NWA 998 and by a factor of ~100 for MIL, in spite of similarities in activation energies. These differences in D/a^2 probably occur because of differences in plagioclase mean grain size between nakhlites and shergottites. In shergottites, plagioclase is a major mineral whose grain size can reach millimeters. Values of D/a^2 in these shergottites are probably controlled by the grain size of the prepared mineral separates. In nakhlites, plagioclase is a fine-grained, minor component and only occurs in the mesostasis interstitial to cumulus augite and olivine (McKay et al. 2006; Mikouchi et al. 2006). Thus, D/a^2 in nakhlites is probably controlled by actual mineral grain sizes. MIL 03346 is the finest-grained among known nakhlites, probably the result of its cooling at a shallow depth, and K is mainly hosted in fine-grained mesostasis, not plagioclase (McKay et al. 2006; Mikouchi et al. 2006). Faster ^{39}Ar diffusion in MIL 03346 compared to the other two nakhlites most probably is the result of the K phases in MIL 03346 possessing even smaller grain sizes, and significantly smaller than the grain size range of the mineral separates analyzed.

Figure 8 compares Ar diffusion characteristics in plagioclase and pyroxene separates of Martian meteorites with whole rock samples of a eucrite (Yamaguchi et al. 2001), a mesosiderite (Bogard and Garrison 1998b), and a H-5 chondrite (Bogard et al. 2001), all JSC data. Potassium in the three non-Martian meteorites is primarily contained in plagioclase. These three non-Martian meteorites show activation energies (Arrhenius slopes) similar to those for nakhlite plagioclase and Y-00097 plagioclase, but slightly greater than activation energies shown by some other shergottites, such as Zagami. At a given temperature, the values of D/a^2 for the eucrite and the mesosiderite are slightly smaller than those for the nakhlites and most shergottites, whereas values of D/a^2 for this chondrite are similar to those for nakhlites. This data comparison suggests that Ar diffusion characteristics in plagioclases of a wide variety of meteorites, including Martian meteorites, are generally similar, especially in the temperature range of 800–1100 °C. We would expect Ar diffusion in Martian rocks to behave similarly.

ARGON DEGASSING REQUIREMENTS

The Ar diffusion data presented in Figs. 5–7 for Martian shergottites and nakhlites permit us to predict the amount of heating that would be required to quantitatively degas both radiogenic ^{40}Ar and cosmogenic Ar from similar Martian rocks. The fractional loss of Ar can be related to both the value of D/a^2 at a given temperature and the elapsed time at that temperature (Lagerwall and Zimen 1964; Fechtig and Kalbitzer 1966; Park et al. 2008). Figure 9 plots values of D/a^2 against time, where the diagonal lines represent various fractional losses of Ar, ranging from 10% to 99%. If we anticipate that a robotic craft on Mars could probably heat a rock sample to a temperature of 900–1000 °C (D. Ming, personal communication), this temperature range defines a range of D/a^2 values for the plotted diffusion data in Figs. 5–7. The horizontal bands in Fig. 8 represent this range of D/a^2 values for ^{40}Ar diffusion in six shergottite plagioclases, ^{40}Ar diffusion in the three nakhlite plagioclases, and ^{37}Ar and cosmogenic Ar diffusion in shergottite and nakhlite pyroxenes. Where these horizontal bands intersect the diagonal line for 99% gas loss defines, on the X-axis, the required heating time at that temperature. To extract 99% of ^{40}Ar from these shergottites at 900–1000 °C would require heating times of ~3–30 h. Heating these plagioclases to 1000 °C for one hour would degas only ~60–70% of their total ^{40}Ar. To extract 99% of ^{40}Ar from these three nakhlites at 900–1000 °C would require heating times of only a few minutes for MIL to almost an hour for the other two nakhlites. To extract 99% of cosmogenic Ar from shergottite pyroxenes at 900–1000 °C would require heating times of 1–13 days. Extracting Ar from nakhlite pyroxenes might require heating times of ≥1 year.

Obviously, the long heating times required to quantitatively (99%) extract Ar from some of these samples is impractical. We can arbitrarily define a sample heating time of 15 min and use the same data to examine the fraction of total Ar that would be degassed as a function of temperature, as is shown in Fig. 10. A 15 min heating of all three nakhlites to 1000 °C could degas ~90% or more of ^{40}Ar, but would degas <10% of the cosmogenic Ar from nakhlite pyroxene. Heating the shergottites for 15 min. to 1000 °C would degas ~50% of the ^{40}Ar, but ~15% of cosmogenic Ar in pyroxene. The fraction of ^{40}Ar degassed from plagioclase in both shergottites and nakhlites increases relatively rapidly with increasing temperature for temperatures between ~600–1200 °C, but the fractional Ar degassing for pyroxenes is less sensitive to increasing temperature. This results because of the much larger activation energies for Ar diffusion in pyroxene compared to feldspar.

From the predictions of required sample heating temperatures and times given by Figs. 9 and 10, extracting ^{40}Ar from these nakhlites on Mars may be feasible, extracting ^{40}Ar quantitatively from these shergottites would be difficult, and extracting cosmogenic Ar quantitatively from these pyroxenes would be exceedingly difficult. For ^{40}Ar, higher fractions of Ar extraction would occur at higher heating temperatures. However, given likely constraints on power in a robotic craft, heating to 1200 °C for a significant time would seem to present a difficult problem. Another variable in extracting Ar is grain size, which controls diffusion distance before gas loss. Thus, in the D/a^2 parameter, decreasing diffusion distance, a, by a factor of two decreases D/a^2 by a factor of four, and the required heating time decreases proportionally. Thus, if we assume the 111 micron mean grain size of our shergottite mineral separates represents the Ar diffusion distance, grinding a similar Martian rock to ~55 microns or ~23 microns would decrease the required heating times for quantitative Ar extraction by factors of 4 and 16, respectively. Grinding is an option that should be investigated for any robotic mission attempting to quantitatively extract Ar from igneous Martian rocks.

CONCLUSIONS

Performing K-Ar age dating of igneous rocks on Mars by robots presents technical challenges. Some of these can be defined by examining Ar-Ar data acquired on Martian meteorites, and others can be evaluated through simulation of possible K-Ar isochrons that could be acquired on Martian rocks. Shergottite meteorites almost all contain an excess ^{40}Ar component that cause the apparent K-Ar age to be too old. This may be a common property among Martian rocks. Thus, the slope of K-Ar isochrons, which cannot be assumed to pass through the origin, must be determined to some given precision for an age to be both precise and accurate. Use of ^{36}Ar to normalize such isochrons can result in significant scattering because of the presence of multiple ^{36}Ar components (Bogard and Park 2008a). Isochrons of total K versus total ^{40}Ar should also be examined. To define an isochron, normalized to ^{36}Ar or not, it is desirable to analyze multiple samples of the same age, but having a range in K concentrations. A 50% K range for 10 such sample analyses may be satisfactory, if the analytical measurement precisions for K and Ar are low, on the order of 3%. If analytical measurement precision is larger, say 10%, then the range in K among 10 samples should be a factor of 2 or more. Increasing the number of analyzed samples of the same age is less important in the derived precision of the age as is the precision of the measurements and range in K concentrations.

Ar diffusion data derived from Ar-Ar dating of Martian shergottites and nakhlites demonstrate that quantitative extraction of Ar from igneous rocks on Mars may be very difficult, given likely power limitations for heating the samples. To quantitatively extract radiogenic ^{40}Ar from shergottites and nakhlites at heating temperatures of 900–1000 °C would require heating times ranging from a few min (one nakhlite) to many hours (several shergottites). Much of the cosmogenic Ar in a Martian rock is contained in mafic phases, and Ar diffusion in pyroxene is slower by orders of magnitude compared to Ar diffusion in plagioclase. To have any hope of quantitatively extracting cosmogenic Ar from these meteorites would require either considerably higher heating temperatures or grinding the samples to smaller grain sizes to significantly increase Ar diffusion rates. Sample grinding should be examined as an option for any attempt at robotic K-Ar dating of igneous rock.

Acknowledgments—I thank Chi-Yu Shih for furnishing mineral separates prepared for radiometric dating and Jisun Park and Dan Garrison for participating in the Ar-Ar analyses. Funding was provided by NASA's Cosmochemistry Program. Valuable reviews were provided by Vera Fernandes, Tim Swindle, and an anonymous reviewer.

Editorial Handling—Dr. Timothy Swindle

REFERENCES

Anonymous. 2008. Generate Gaussian random numbers. http://www.helpdesk.graphpad.com.

Bogard D. D. and Johnson P. 1983. Martian gases in an Antarctic meteorite. *Science* 221:651–654.

Bogard D. D. and Garrison D. H. 1998a. Relative abundances of argon, krypton, and xenon in the Martian atmosphere as measured in Martian meteorites. *Geochimica et Cosmochimica Acta* 62:1829–1835.

Bogard D. D. and Garrison D. H. 1998b. ^{39}Ar-^{40}Ar ages and thermal history of mesosiderites. *Geochimica et Cosmochimica Acta* 62: 1459–1468.

Bogard D. D. and Garrison D. H. 1999. ^{39}Ar-^{40}Ar "ages" and trapped argon in Martian shergottites, Chassigny, and Allan Hills 84001. *Meteoritics & Planetary Science* 34:451–473.

Bogard D. D. and Park J. 2008a. ^{39}Ar-^{40}Ar dating of the Zagami Martian shergottite and implications for magma origin of excess ^{40}Ar. *Meteoritics & Planetary Science* 43:1113–1126.

Bogard D. D. and Park J. 2008b. Excess ^{40}Ar in Martian shergottites, K-^{40}Ar ages of nakhlites, and implications for in situ K-Ar dating of Mars' surface rocks (abstract #1100). 39th Lunar and Planetary Science Conference. CD-ROM.

Bogard D. D., Garrison D. H., and Masarik J. 2001. The Monahans chondrite and halite: ^{39}Ar-^{40}Ar age, solar gases, cosmic-ray exposure ages, and parent body regolith neutron flux and thickness. *Meteoritics & Planetary Science* 36:107–122.

Carter E. F. 2008. Generating Gaussian random numbers. http://www.taygeta.com.

Fechtig H. and Kalbitzer S. 1966. The diffusion of argon in potassium-bearing solids. In *Potassium-argon dating*. Berlin: Springer-Verlag. pp. 68–107.

Fritz J., Artemieva N., and Greshake A. 2005. Ejection of Martian meteorites. *Meteoritics & Planetary Science* 40:1393–1411.

Ikeda Y., Kimura M., Takeda H., Shimoda G., Kita N. T., Morishita Y., Suzuki A., Jagoutz E., and Dreibus G. 2006. Petrology of a new basaltic shergottite: Dhofar 378. *Antarctic Meteorite Research* 19: 20–44.

Lagerwall T. and Zimen K. E. 1964. The kinetics of rare-gas diffusion in solids. EURAEC Report No. 772 (Report of European Atomic Energy Community).

Marti K., Kim J. S., Thakur A. N., McCoy T. J., and Keil K. 1995. Signatures of the Martian atmosphere in glass of Zagami meteorite. *Science* 267:1297–1305.

Mathew K. J. and Marti K. 2001. Early evolution on Martian volatiles: Nitrogen and noble gas components in ALH 84001 and Chassigny. *Journal of Geophysical Research* 106:1401–1422.

McKay G., Mikouchi T., and Schwandt C. 2006. Additional complexities in nakhlite pyroxenes: A progress report (abstract #2435). 37th Lunar and Planetary Science Conference. CD-ROM.

McSween H. Y. 1994. What we have learned about Mars from SNC meteorites. *Meteoritics* 29:757–779.

McSween H. Y. 2002. The rocks of Mars, from far and near. *Meteoritics & Planetary Science* 37:7–25.

Mikouchi T., Miyamoto M., Koizumi E., and McKay G. 2006. Relative burial depths of nakhlites: An update (abstract #1865). 37th Lunar and Planetary Science Conference. CD-ROM.

Misawa K., Park J., Shih C., Reese Y., Bogard D., and Nyquist L. 2008. Rb-Sr, Sm-Nd, and Ar-Ar isotopic systematics of lherzolitic shergottite Yamato-000097. *Polar Science* 2:163–174.

Neukum G. and Hartmann W. K. 2001. Cratering chronology and the evolution of Mars. *Space Science Reviews* 96:165–194.

Nyquist L. E., Borg L. E., and Shih C.-Y. 1998. The shergottite age paradox and the relative probabilities for Martian meteorites of differing age. *Journal of Geophysical Research* 103:31,445–31,455.

Nyquist L. E., Bogard D. D., Shih C. Y., Greshake A., Stöffler D., and Eugster O. 2001. Ages and geologic histories of Martian meteorites. *Space Science Reviews*. 96:105–164.

Park J., Garrison D., and Bogard D. 2007. ^{39}Ar-^{40}Ar ages of two nakhlites, MIL 03346 and Y-000593: A detailed analysis (abstract #1114). 38th Lunar and Planetary Science Conference. CD-ROM.

Park J., Bogard D. D., Mikouchi T., and McKay G. A. 2008. The Dhofar-378 Martian shergottite: Evidence of early partial melting. *Journal of Geophysical Research* 113, E08007.

Schwenzer S. P., Herrmann S., Mohapatra R. K., and Ott U. 2007. Noble gases in mineral separates from three shergottites: Shergotty, Zagami, and EETA79001. *Meteoritics & Planetary Science* 42:387–412.

Swindle T. D. 2001. Could in situ dating work on Mars? (abstract #1492). 32nd Lunar and Planetary Science Conference. CD-ROM.

Swindle T. D. and Olson E. K. 2004. ^{40}Ar-^{39}Ar studies of whole rock nakhlites: Evidence for the timing of formation and aqueous alteration on Mars. *Meteoritics & Planetary Science* 39:755–766.

Terribilini D., Eugster O., Burger M., Jakob A., and Krähenbühl U. 1998. Noble gases and chemical composition of Shergotty mineral fractions, Chassigny, and Yamato-793605: The trapped ^{40}Ar/^{36}At ratio and ejection times of Martian meteorites. *Meteoritics & Planetary Science* 33:677–684.

Turner G., Enright M. C., and Cadogan P. H. 1978. The early history of chondrite parent bodies inferred from ^{40}Ar-^{39}Ar ages. Proceedings, 9th Lunar and Planetary Science Conference. pp. 989–1025.

Turner G., Knott S. F., Ash R. D., and Gilmour J. D. 1997. Ar-Ar chronology of the Martian meteorite ALH 84001: Evidence for the timing of the early bombardment of Mars. *Geochimica et Cosmochimica Acta* 61:3835–3850.

Walton E. L., Kelley S. P., and Spray J. G. 2007. Shock implantation of Martian atmospheric argon in four basaltic shergottites: A laser probe ^{40}Ar/^{39}Ar investigation. *Geochimica et Cosmochimica Acta* 71:497–520.

Williamson J. H. 1968. Least-squares fitting of a straight line, *Canadian Journal of Physics* 46:1845–1847.

Yamaguchi A., Taylor G. J., Keil K., Floss C., Crozaz G., Nyquist L. E., Bogard D. D., Garrison D. H., Reese Y., Wiesmann H., and Shih C. Y. 2001. Post-crystallization reheating and partial melting of eucrite EET 90020 by impact into the hot crust of asteroid 4 Vesta ~4.50 Gyr ago. *Geochimica et Cosmochimica Acta* 65:3577–3599.